Hierarchically Ordered Macro-/Mesoporous Silica Monolith: Tuning Macropore Entrance Size for Size-Selective Adsorption of Proteins

ARTICLE *in* CHEMISTRY OF MATERIALS · MARCH 2011

Impact Factor: 8.35 · DOI: 10.1021/cm103704s

CHEMISTRY OF MATERIALS

ARTICLE

pubs.acs.org/cm

Hierarchically Ordered Macro-/Mesoporous Silica Monolith: Tuning Macropore Entrance Size for Size-Selective Adsorption of Proteins

Zhenkun Sun, Yonghui Deng,* Jing Wei, Dong Gu, Bo Tu, and Dongyuan Zhao*

Department of Chemistry and Shanghai Key Lab of Molecular Catalysis and Innovative Materials, Laboratory of Advanced Materials, Fudan University, Shanghai 200433, P. R. China

Supporting Information

ABSTRACT: In this paper, hierarchically ordered macro-/meso porous silica monoliths with 3D fcc packed macropores and 2D hexagonally arranged mesopores are synthesized by using polymer colloidal crystals as the hard template and block copolymer Pluronic P123 as a soft template. Through the impregnation of the colloidal crystal hard template with an acidic ethanol solution containing silica source and P123, the entrance size of macropores can be tailored by controlling the synthesis conditions. As the acid concentration increases, the resulting mesopore sizes tend to decrease slightly in the range of 4.7−3.6 nm, meanwhile, the macropore entrance size increase gradually from 0 to ca. 200 nm. These highly ordered macro-/mesoporous silica monoliths have a macropore of about 1.0 μm with tunable window size (0−200 nm), high surface area (ca. 330 m^2/g) and large pore volume (∼ 0.36 cm^3/g). Biomacromolecule adsorption results show that the porous silica monolith with the macropore entrance of about 50 nm has absorption capacity of ∼16.6 mg/g for bovine serum albumin (BSA, ∼10 nm in size), much higher than that (∼3.4 mg/g) of the porous silica materials without macropore entrance, and the porous materials with or without macropore entrances exhibit similar a adsorption capacity for cytochrome *c* (Cyt.c, dimension: ∼ 3 nm) (∼36.8 mg/g), suggesting that the large guest molecules can be excluded by the porous silica monoliths without the macopore entrances. These results indicate that, through engineering the pore connection and multimodal pore system, porous materials with hierarchically pores and tailorable window sizes can be created for size-selective applications, such as enrichment, nanofiltration, and drug delivery.

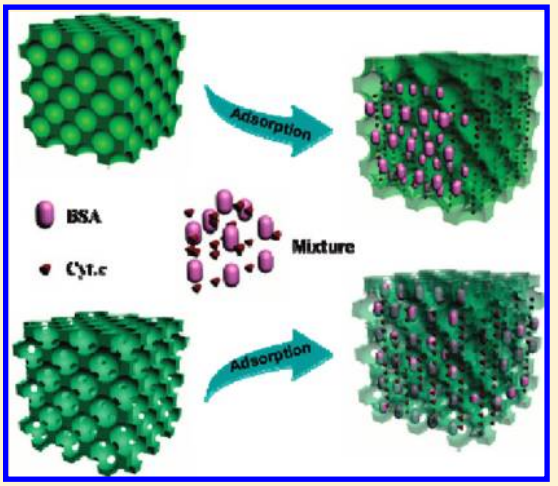

KEYWORDS: porous materials, self-assembly and self-assembled materials, sol−gel chemistry/processing

1. INTRODUCTION

Ever since its discovery,[1−7] ordered mesoporous material, as an intriguing porous material, has attracted considerable attention because of its open pore structure, uniform pore size, and large pore volume, and as a result, diverse potential applications in catalysis, adsorption, sensors, and biotechnologies. Mesoporous materials are usually synthesized through a sol−gel process with small molecular surfactants or amphiphilic block copolymers as structure-directing agents.[8−11] By using different strategies, researchers are now able to synthesize various kinds of mesoporous materials with controllable morphologies, framework compositions, pore structures and pore sizes. Although mesopores provide high surface areas and shape-selectivity for guest molecules, they exhibit considerable resistance of diffusion especially in the case of long transportation distance due to pore size limitation. So far most of the reported mesoporous materials synthesized using the above methods possess pore size of less than 30 nm with entrance size smaller than 6 nm, which may limit their practical applications involving large molecule transportation, such as protein enrichment, separation, and enzymolysis of biomolecules.[12]

Through the templating approaches based on polymer latexes,[13−15] silica spheres,[16] and organic emulsions as templates,[17] three-dimensionally (3D) ordered macroporous materials with pore size ranging from tens of nanometers to several micrometers and large window size (usually from tens of nanometers to several hundred nanometers) can be readily synthesized. Because of their large interconnected pores, these macroporous materials can provide excellent performance of mass transport and offer easier accessibility for guest objects, but their surface area is relatively lower which is disadvantageous for efficient adsorption. Therefore, design of porous materials with both high surface area and efficient mass transportation is desired in practical applications. Over the past years, enlightened by the universal existence of hierarchically ordered pore structures in nature (e.g., diatoms, lumbar vertebra, and lungs) that offer efficient transport of fluids and gases,[18−20] much work has been

Received: December 30, 2010
Revised: March 15, 2011
Published: March 25, 2011

Scheme 1. (a) Synthesis Procedure for the Ordered Macro-/Mesoporous Silica Monoliths with Controllable Macroporous Entrances and (b) Their Application for Size Selective Absorption of Biomolecules in the Mixture of BSA and Cyt.c

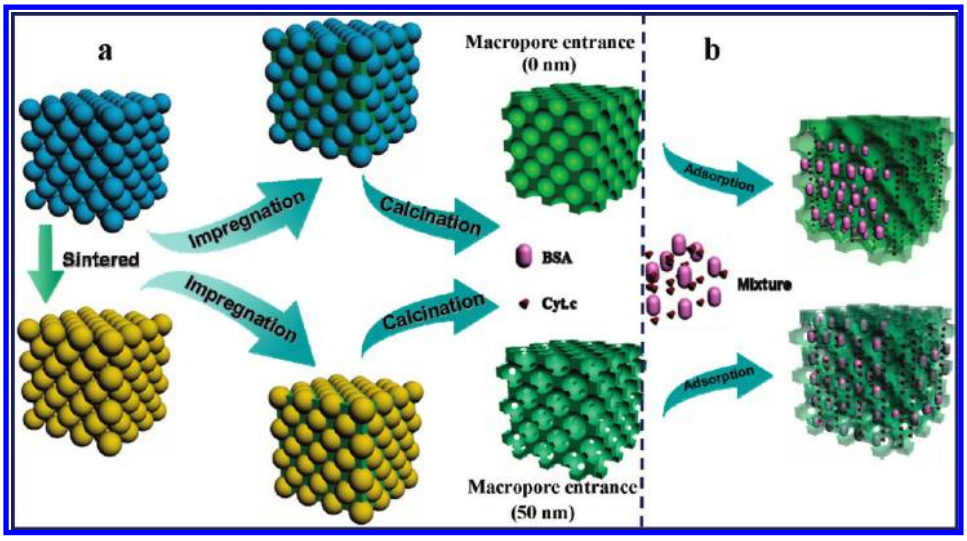

reported to design hierarchically ordered porous materials that combine mesopores with macropores and have various framework compositions, including silica, carbon, or metal oxides. The hierarchically ordered porous materials can allow the reactant molecules to diffuse more easily in the entire bimodal pore system through the macropore windows which make the mesopores interconnected. Until now, although considerable work has been reported on the synthesis of hierarchically ordered macro-/mesoporous materials via colloidal crystal and surfactant dual templating,[21−28] most of them focus on the regulation of framework composition the shape or alignment of mesopores.[29,30] No work has been done to synthesize hierarchically ordered meso/macroporous materials with finely tunable macropore entrance size. Tuning the macropore window size is very important to the control of the mass transportation in the porous system for size-selective enrichment and separation of biomolecules with different size from complex system.

In this paper, we demonstrate a dual-template approach to synthesize hierarchically ordered meso-/macroporous silica monolith with controllable macropore window sizes. Since silica is a bioinert material and can be easily modified with various functionalities, the hierarchically ordered meso-/macroporous silica monolith could be applied to various bioseparation processes with specific selectivity. Here, homemade poly(St-*co*-TMSPM) latex spheres and amphiphilic triblock copolymers (Pluronic P123) were employed as a hard template and a soft template, respectively. By controlling the synthesis conditions including the prehydrolysis degree of the silica source, the concentration of acid and the sintering temperature, hierarchically ordered porous silica monoliths with 3D ordered arrays of macropore (1.0 μm), controllable macropore entrance sizes (0−200 nm), and 2D hexagonally aligned mesopores (3.5−4.6 nm), high surface area (300−500 m^2/g) and large pore volume (0.34−0.48 cm^3/g) were successfully obtained. According to the absorption experiments with bovine serum albumin (BSA, ∼14 nm in size) and Cytochrome *c* (Cyt.c, ∼3 nm) as the model biomacromolecules, the porous silica monolith with macropore entrance of about 50 nm has adsorption capacity of ∼16.6 mg/g for BSA much higher than that (∼3.4 mg/g) of the porous silica monolith without the macropore entrance, but both the porous silica monoliths with or without macropore entrance shows similar adsorption capacity (∼37 mg/g) for Cyt.c, suggesting that it can effectively exclude the biomacromolecules with large size, namely, showing an excellent size selectivity in bioadsorption. These results indicate that, through engineering the pore connection and multimodal pore system, porous materials with hierarchical pores and tailorable window sizes can be created for size-selective applications, such as enrichment and separation, drug delivery and nanofiltration.

2. EXPERIMENTAL SECTION

2.1. Chemicals. 3-(Trimethoxysilyl)propyl methacrylate (TMSPM) polyvinylpyrrolidone (PVP, M_w = 30000) was purchased from Aldrich and used as received. 2,2-Azobisisobutyronitrile (AIBN) (Acros) was recrystallized in methanol before use. Styrene (St), ethanol, concentrated HCl, and tetraethyl orthosilicate (TEOS) were purchased from Shanghai Chem. Corp. The polymerization inhibitor was removed from the styrene by infiltration through Al_2O_3 column. Distilled water was used in this study.

2.2. Preparation of Poly(St-co-TMSPM) Colloidal Crystals. Monodisperse poly(St-co-TMSPM) microspheres with a mean size of ∼1.2 μm were prepared through a dispersion polymerization approach.[31] A detailed description of synthetic procedure for poly(St-co-TMSPM) microspheres is shown in the Supporting Information. The resulting polymer microspheres were repeatedly washed with an ethanol−water mixture (1: 1 volume ratio) by centrifugation and then redispersed in water to obtain a colloidal solution. Finally, an aqueous dispersion (40 g) of poly(St-co-TMSPM) microspheres (5 wt % solid content) was let to stand for a week to form a closely packed colloidal crystal at the bottom of the vessel by gravity sedimentation. After careful removal of the supernatant liquid and further drying at 25 °C for 48 h, the as-made colloidal crystals were produced and could be directly used as the hard template for macro-/mesoporous silica monoliths. In some cases, the as-made colloidal crystals were sintered at different temperature (80 or 90 °C) and time (12 or 24 h) and then used for the templating synthesis of macro-/mesoporous silica monoliths.

2.3. Preparation of Hierarchically Ordered Porous Silica. The hierarchically ordered porous silica monoliths (denoted as HOPS) were prepared through a dual-templating synthesis approach with 3D

Table 1. Synthesis Conditions of the Hierarchically Ordered Porous Silicas

samples	2 M HCl (g)	prehydrolysis time (h)	sintering temperature (°C)	sintering time (h)	macropore entrance size (nm)	mesopore size (nm)[a]	BET surfacearea (m^2/g)	total pore volume (cm^3/g)
HOPS-80-12 h [b]	0.1	1	80	12	0	4.4	299	0.34
HOPS-80-24 h [b]	0.1	1	80	24	0	4.6	249	0.29
HOPS-90-12 h [b]	0.1	1	90	12	150	4.2	496	0.48
HOPS-90−24 h [b]	0.1	1	90	24	155	3.4	296	0.25
HOPS-01-01 [c]	0.1	1			0	4.7	314	0.39
HOPS-03-01 [c]	0.3	1			0	3.8	399	0.41
HOPS-05-01 [c]	0.5	1			0	3.6	380	0.34
HOPS-08-01 [c]	0.8	1			50	3.6	316	0.29
HOPS-08-10 [d]	0.8	10			80	4.2	385	0.43
HOPS-08-20 [d]	0.8	20			200	3.5	364	0.33

[a] Determined from the adsorption branch on the basis of the BJH model. [b] Templated by polymercolloidal crystals sintered at different temperatures for a certain time. [c] Prepared with different amounts of 2.0 M HCl. [d] Prepared by increasing the prehydrolysis time of TEOS.

ordered poly(St-co-TMSPM) colloidal crystals as a hard template and amphiphilic triblock copolymer Pluronic P123 as a soft template, and TEOS as the silica source (Scheme 1). First, the precursor sol was prepared by mixing Pluronic P123, ethanol, H_2O, TEOS and various amounts of 2.0 M HCl solution (0.1, 0.3, 0.5, or 0.8 g) for certain time (1, 10, or 20 h) (see Table 1) under magnetic stirring at room temperature. Second, the colloidal crystal monoliths were impregnated with the above solution to introduce the P123-silica composites into the interstitial voids. Finally, the hierarchically ordered silica materials were obtained by calcination of the impregnated colloidal crystals. In a typical preparation procedure, a piece of colloidal crystal monoliths (1.0 g) with a dimension of ca. 1 × 1 × 0.5 cm^3 was immersed in 17.0 g of a homogeneous silicate precursor solution obtained by mixing TEOS (2.08 g), H_2O (0.9 g), 2.0 M HCl (0.1 g), P123 (1.0 g) and ethanol (15 g) for 1 h. After the impregnation and evaporation for 48 h at 30 °C, the composite monolith was carefully scratched with a blade to remove excess gel precursor and taken out to evaporate remnant ethanol completely at 40 °C for another 4 h. Finally, the impregnated colloidal crystal was calcined in air at 550 °C for 6 h at heat rate of 1 °C/min to remove polymer microspheres and P123 templates, and a monolith of hierarchically ordered porous silica (HOPS-01-01) with macroporosity and mesoporosity was obtained. By using the colloidal crystals without sintering as the hard template, a series of samples were synthesized and designated as HOPS-*x*-*y*, wherein *x* and *y* refers to the amount (g) of 2.0 M HCl solution and prehydrolysis time (h), respectively. Similarly, by using sintered poly(St-co-TMSPM) colloidal crystals as the hard template, a series of samples were synthesized and designated as HOPS-*m*-*n*, wherein *m* and *n* refer to the sintering temperature (°C) and sintering time, respectively.

2.4. Protein Adsorption. To investigate the size selectivity of the hierarchically ordered porous silica in adsorption, HOPS-08-01 with macropore entrance size of about 50 nm and HOPS-01-01 without macropore entrance were chosen as absorbents (Scheme 1). Two proteins with different hydrodynamic sizes, Bovine serum albumin (BSA, MW. 66,000 Da, Shanghai Chem. Corp.) and cytochrome c (Cyt.c, MW. 13,750 Da, Sigma-Aldrich) were employed as model guest molecules for the adsorption experiments. Three protein solutions, i.e., BSA, Cyt.c, and mixture of BSA and Cyt.c were prepared in NaOH/$NaHCO_3$ buffer solution (pH 9.5) and used for the adsorption tests. First, 0.020 g of HOPS sample was added to 20 mL of BSA (100 mg/L) or 10 mL of Cyt.c aqueous solution (80 mg/L), respectively. The mixed solution was then vibrated at room temperature for 6 h, and subjected to gentle centrifugation (1000 rpm). The supernatant was used for UV−vis spectroscopy measurements. The characteristic absorption peak was selected at 280 nm for BSA and 409 nm for Cyt.c, respectively.[34−39] Standard curves were drawn by measuring a series of BSA aqueous solutions with concentrations of 20−100 mg/L and Cyt.c of 10−80 mg/L. Second, 0.020 g of the HOPS sample was added to an aqueous solution containing 10 mL of BSA (100 mg/L) and 10 mL of Cyt.c solution (80 mg/L) respectively. The mixed solution was then vibrated at room temperature for 6 h. After that, the solution with HOPS monolithic particles was subjected to gentle centrifugation (1000 rpm), and the supernatant was subjected to analysis by SDS-polyacrylamide gel electrophoresis (SDS-PAGE). SDS-PAGE was carried out on a vertical polyacrylamide gel system at a constant voltage of 60 V until the protein bands reached the interface between stacking and separating gels. Separation was performed at a constant voltage of 120 V. The electrophoresis was stopped when the tracker dye (bromophenol) was ca. 1 cm above the end of the glass plates. In order to investigate the adsorption performance of HOPS materials, a series of Cyt.c solutions with concentrations of 0.01−0.5 g/L were prepared by using NaOH/$NaHCO_3$ buffer solution (pH 9.5) for adsorption isotherms. For each adsorption experiment, 0.02 g of HOPS-08-01 samples was added into 5 mL of Cyt.c solution, followed by shaking at room temperature for 6 h. Using UV−vis spectra measurement, the adsorption amount of Cyt.c was calculated by subtracting the in the supernatant liquid after adsorption from the initial amount of Cyt. c in the solution before addition of HOPS sample.

2.5. Characterization and Measurements. Scanning electron microscopy (SEM) images were recorded on a Philips XL30 electron microscope (Netherlands) operating at 20 kV. A thin gold film was sputtered on the sample before characterization. Transmission electron microscopy (TEM) images were taken with a JEOL 2011 microscope (Japan) operating at 200 kV. For the TEM measurements, the samples were dispersed in ethanol and then dried on a holey carbon film Cu grid. Small-angle X-ray scattering (SAXS) measurements were taken on a Nanostar U small-angle X-ray scattering system (Bruker, Germany) using Cu Kα radiation (40 kV, 35 mA). The *d*-spacing values were calculated by the formula $d = 2\pi/q$, wherein q is the scattering vector. Nitrogen sorption isotherms were measured at 77 K with a Micromeritics Tristar 3000 analyzer (USA). Before measurements, the samples were degassed in a vacuum at 160 °C for at least 6 h. The Brunauer−Emmett−Teller (BET) method was utilized to calculate the specific surface areas. By using the BJH model, the pore volumes and pore size distributions were derived from the adsorption branches of isotherms, and the total pore volumes (Vt) were estimated from the adsorbed amount at a relative pressure P/P_0 of 0.992. The instrumental setup for SDS-PAGE consisted of a Mini-PROTEAN 3 electrophoresis chamber connected to an electrophoresis power supply (Bio-Rad, Hercules, CA). SDS-Polyacrylamide Gel Electrophoresis (SDS-PAGE) was performed using 1 mm thickness 12% Tris-Glycine polyacrylamide

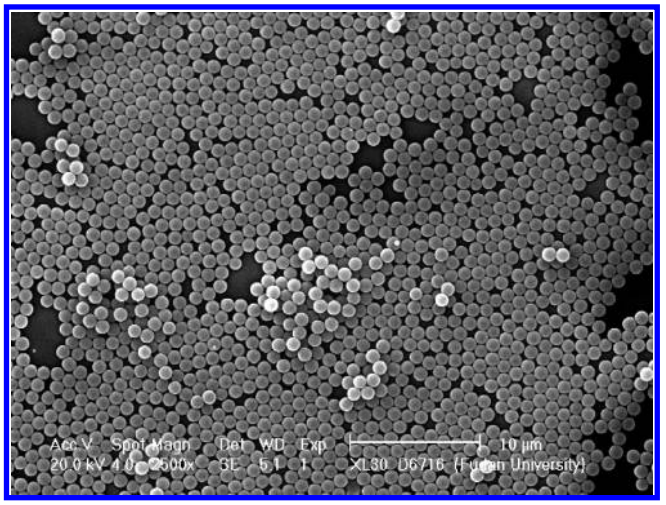

Figure 1. SEM image of poly(St-*co*-TMSPM) microspheres prepared via a dispersion polymerization.

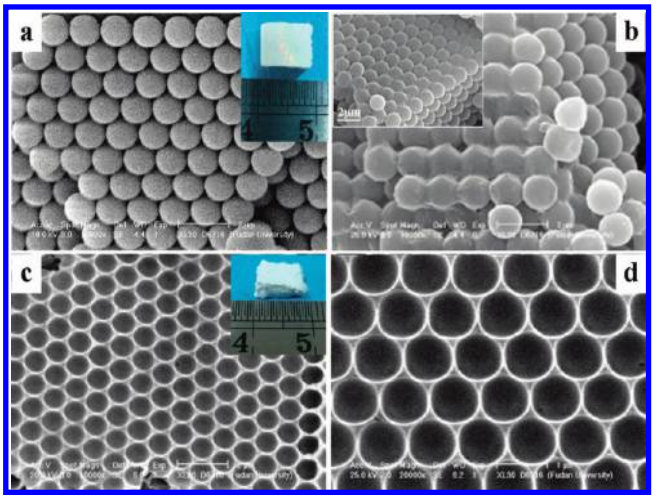

Figure 2. SEM images of (a) the as-made poly(St-*co*-TMSPM) colloidal crystals, (b) the poly(St-*co*-TMSPM) colloidal crystals after the impregnation, (c) the hierarchically ordered porous silica (HOPS-01-01) after the removal of polymer microspheres and P123 templates, and (d) SEM image of c with large magnification. The insets in a and c are the photographs of the colloidal crystal monoliths and the replicated hierarchically ordered porous silica (HOPS-01-01), respectively. The inset in (b) shows the 3D structure of the impregnated poly(St-*co*-TMSPM) colloidal crystals.

minigels, loaded with 1 μg of protein. Following electrophoresis, the gel slab was stained with colloidal Coomassie blue for 4 h, followed by destaining in water overnight.

3. RESULTS AND DISCUSSION

3.1. Tuning the Macropore Window Size. The as-prepared poly(St-*co*-TMSPM) microspheres have a mean diameter of ~1.2 μm with a standard size deviation of less than 5%, as determined from the SEM image (Figure 1). The uniformity of size favors the ordered alignment of the polymer microspheres during the sedimentation. After the sedimentation, the polymer microspheres pack into highly ordered colloidal crystals with face-centered cubic (fcc) structure and the (111) planes parallel to the substrate (Figure 2a, inset). As a result of the ordered structure, the colloidal crystal monolith shows pearlescent color due to the light diffraction (Figure 1a inset). After the impregnation with the acidic P123/TEOS/ethanol solution and solvent evaporation process, the interstitial voids in the as-made colloidal crystals can be filled by P123/silica composites, and gel-like species around the microspheres can be visible in the SEM image (Figure 2b); meanwhile, the 3-D ordered colloidal crystal structure is well retained (Figure 2b, inset). After further calcination in air at 500 °C, the block copolymer P123 and the polymer microspheres can be removed, and white monolith (HOP-01-01) with 3D ordered macroporous structure is obtained (Figure 2c, inset), indicating that the ordered structure of colloidal crystals is faithfully replicated. Compared with the colloidal crystal template (Figure 1a), the HOP-01-01 sample shows similar external morphology but smaller dimension (ca. 15% shrinkage) because of the removal of the polymer microspheres and condensation of the silica framework. Notably, different from most previous reports,[31] the HOP-01-01 sample does not show clear macropore entrances even in high-magnification SEM image (Figure 2d), which means that the macropore window in the HOP-01-01 sample is closed.

The formation of separated macropores of HOP-01−01 sample may be due to the fact that the as-made colloidal crystals obtained after drying at room temperature was directly used for the hard-templating synthesis of the sample HOPS-01−01, and the contact area between the neighboring microspheres is very small. When being soaked in the sol solution, the polymer microspheres in the colloidal crystals can be swelled by TEOS due to hydrophobic interaction, and this can lead to a slightly *in situ* expansion of the colloidal crystals in ethanol solution. The microspheres in the colloidal crystals can be fully surrounded with sol solution during the impregnation. After the impregnation and subsequent solvent evaporation, the mesostructured P123/silica composites can coat the polymer microspheres and fill up the interstitial voids in the colloidal crystals. Removal of polymer microspheres and P123 templates by calcination in air results in a 3-D ordered macroporous silica monolith with separated macropores.

3.1.1. Effect of HCl Amount. By impregnation of the as-made colloidal crystal monolith in the precursor solution obtained using different amount of 2.0 M HCl solution (0.1−0.8 g), a series of hierarchically ordered meso-/macroporous silica monoliths (HOPS-*x*-*y*) can be synthesized. As shown in the respective SEM images (Figure 3), all the samples exhibit 3D ordered macroporous structures. However, similar to HOPS-01-01 (Figure 3a), the HOPS samples (HOPS-03-01, HOPS-05-01) obtained with a larger amount of HCl solution (0.3 and 0.5 g) also possess 3-D ordered macroporous structure without entrances (Figure 3b, c). When the amount of HCl solution increases to 0.8 g, the obtained HOPS-08-01 sample shows ordered macroporous structure with clear entrances of about 50 nm (Figure 3d), indicating the formation of open macropores. It suggests that the acidity of the prehydrolyzed precursor solution plays an important role in controlling the entrance size of the macropores in the 3D ordered hierarchical porous silica monolith.

This distinct change of the macropore entrance size of these samples may result from the difference in the hydrolysis degree of the precursor solutions. In the cases of a low amounts of HCl solution (0.1, 0.3, 0.5 g), the TEOS precursors are not sufficiently hydrolyzed and can swell the polymer microspheres in the

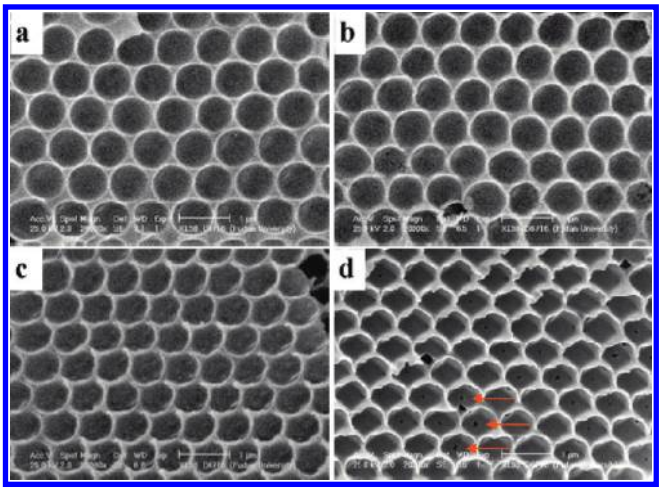

Figure 3. SEM images of the samples (a) HOPS-01−01, (b) HOPS-03−01, (c) HOPS-05−01, and (d) HOPS-08−01. These samples were prepared by using the precursor solution catalyzed with (a) 0.1, (b) 0.3, (c) 0.5, and (d) 0.8 g of 2.0 M HCl solution and after the impregnation for 1 h.

colloidal crystal during the impregnation, making them approachable to the P123 and silica oligomers in the sol solution. In this way, each polymer microsphere in the colloidal crystals can be fully coated by P123-silica composites after the impregnation and solvent evaporation, resulting in a 3D ordered macroporous silica after calcination. When a large amount of HCl solution is used, the precursor solution can be highly hydrolyzed even in short time (1 h), and the polymer microspheres in the colloidal crystals can tightly contact with each other without being swelled during impregnation, and therefore P123-silica composites can not fully cover the microspheres after the impregnation and solvent evaporation, and finally HOPS with accessible macropores is obtained after the calcination.

3.1.2. Effect of the Prehydrolysis Time. Using the precursor solutions obtained with 2.0 M HCl solution (0.8 g) and different prehydrolysis time (1−20 h), a series of hierarchically ordered meso-/macro- porous silica monoliths (HOPS-*m*-*n*) materials were obtained with the as-made colloidal crystal as the hard template. As shown in Figure 4, all the HOPS samples display 3D ordered macroporous structure, suggesting that the prehydrolysis time has no significant influence on the macrostructure. However, the macropore window size dramatically increases from 50 nm for the HOPS-08-01 sample, to 80 nm for HOPS-08-20, and to 200 nm for HOPS-08-20, respectively, as the prehydrolysis time is prolonged from 1 to 20 h. These results indicate that the macropore window size can be readily enlarged by prolonging the prehydrolysis time of the precursor solution before the impregnation of the colloidal crystals.

Similar to the effect of HCl solution, prolonging the hydrolysis time can lower the TEOS content and improve the hydrolysis degree of the silica species in the precursor solution, and this would retard the polymer microspheres from being swollen and in situ disassembled. Therefore, the reduction of contact area between the neighboring polymer microspheres would become negligible during the impregnation, and thus the HOPS samples obtained with precursor longer prehydrolysis time possess larger macropore window sizes.

3.1.3. Effect of Sintering Temperature for the Colloidal Crystals. Sintering treatment of the colloidal crystals prior to the impregnation was also conducted to investigate the influence on the macropore window size. Because the poly(St-*co*-TMSPM) microspheres possess a glass transition temperature (T_g) of 102 °C,[32] the colloidal crystals of the microspheres can be sintered at temperatures slightly lower than 100 °C to prevent them from melting. Figure S1 shows the SEM images of HOPS samples synthesized using colloidal crystal templates treated at 80 or 90 °C for 8 or 12 h and prehydrolyzed precursor sol solution. All the samples show well-ordered 3D macroporous structures; however, only HOPS-90−12 h and HOPS-90−24 h samples using colloidal crystal sintered at 90 °C for 12 and 24 h, respectively, possess large macropore entrances (∼ 150 nm) and the HOPS samples using colloidal crystals treated at 80 °C as templates do not show macropore windows. It suggests that the increase of sintering temperature can help to generate the macropore entrances. However, sintering the colloidal crystals at too high temperature of ∼100 °C can cause the polymer microspheres to melt, which is not favorable for the prehydrolyzed precursor solution to impregnate into the entire colloidal crystals and disadvantageous to further impregnation.

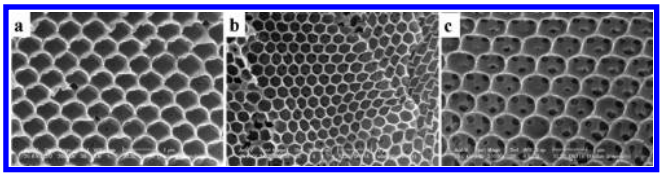

Figure 4. SEM images of the samples (a) HOPS-08−01, (b) HOPS-08−10, and (c) HOPS-08−20 obtained by using the precursor solution catalyzed with 0.8 g of 2.0 M HCl solution and after the impregnation for (a) 1, (b) 10, and (c) 20 h.

The formation of 3D ordered arrays of macropores with open windows are due to the sintering effect. Sintering the colloidal crystals sintered at 90 °C, slightly lower than its *T*g, can make the polymer microspheres partially melt, and the polymer chains at the contact areas entangle with each other. It results in an infrangible contact area between neighboring microspheres, which acts as the basis of the formation of the interconnections (or windows) of macropores in the porous monoliths after the impregnation and calcination. Sintering treatment at 80 °C even for 24 h can not help to form macroporous monolith samples with open windows (see Figure S1a,b in the Supporting Information). Compared to the HOPS-90-12 sample, no significant increase in the macropore window size is observed for the HOPS-90-24 sample obtained by using colloidal crystal sintered at the same temperature but for longer time (see Figure S1c,d in the Supporting Information). These results clearly indicate that the formation of rigid contact areas between the microspheres in the colloidal crystal is mainly a thermodynamically controlled process.

3.2. Structure, Composition, and Porosity. TEM images of the obtained macro-/mesoporous silica materials (HOPS-01-01) show ordered array of macropores of ca. 1.0 μm (Figure 5a, b). The high-magnification TEM images (Figure 5c, d) clearly show the ordered alignment of cylindrical mesopores viewed from the [110] direction of a 2D hexagonal mesostructure. The mesopore size is roughly estimated to be about 5.0 nm from the TEM image. Similarly, TEM observations show that the HOPS samples synthesized under other conditions (e.g., using well-pre-hydrolyzed precursor solution by introducing large amount of HCl solution or prolonging the hydrolysis time, or using

colloidal crystal templating sintered at 90 °C) have similar porous structure with 3D ordered macropores (around 1.0 μm) and 2D hexagonally ordered mesopores (3−4 nm), but the macropores are open with the window sizes ranging from 50−200 nm depending on the specific synthesis conditions. For example, the HOPS-08-20 samples obtained with precursor solution catalyzed by 0.8 g of 2.0 M HCl solution after the prehydrolysis for 20 h shows distinct macropores with open windows of about 200 nm as marked in Figure 5c, and the ordered mesostructure can also be clearly seen in the high magnification TEM image shown in Figure 5d.

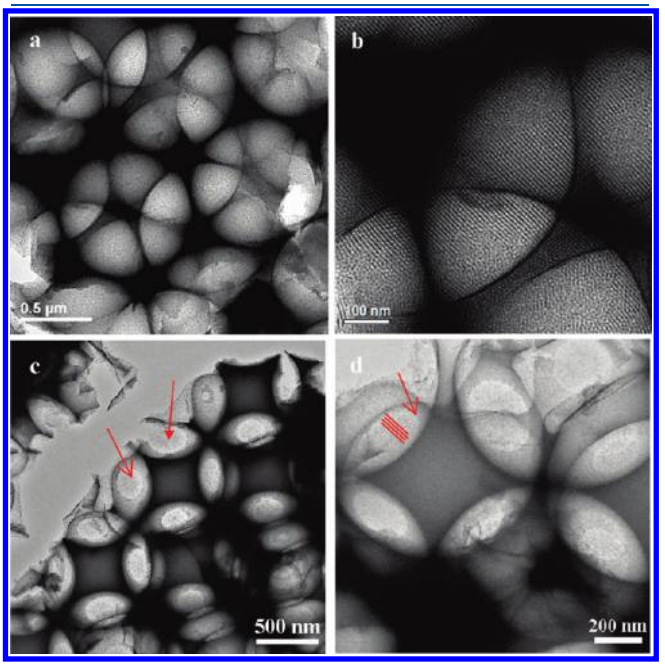

Figure 5. TEM images of the hierarchically ordered porous silica (a, b) HOPS-01-01 without macropore windows obtained by using the as-made polymer colloidal crystals as a template and the precursor solution catalyzed by 0.1 g of 2.0 M HCl solution and after the impregnation for 1 h; (c, d) HOPS-08-20 with macropore size of ∼200 nm obtained by using the as-made polymer colloidal crystals as a template and the precursor solution catalyzed by 0.8 g of 2.0 M HCl solution and after the impregnation for 20 h. High-magnification TEM images (b, d) show the 2D hexagonal arrays of mesopores in both samples.

The framework of the hierarchically ordered macro-/mesoporous silica materials was analyzed by Fourier transfer infrared spectra. The poly(St-*co*-TMSPM) colloidal crystal template (see Figure S2a in the Supporting Information) shows two strong absorption bands at 2800−3100 and 1840−1940 cm^{-1}, both associated with polymer microspheres. The impregnated polymer colloidal crystals (see Figure S2 in the Supporting Information) show absorption bands at 1100−1490 cm^{-1}, which contains the vibration information of ether bonds of P123 and Si−O−Si bonds of silica species. After the calcination, the obtained hierarchically ordered porous silica (see Figure S2c in the Supporting Information) shows absorption bands of silica at 1090 cm^{-1}, absorbed water at 1640 cm^{-1}, and hydroxyl group at around 3500 cm^{-1}, and no band associated with organic species was detected, suggesting the full decomposition of polymer microsphere templates and the surfactant templates. These results demonstrate the successful synthesis of the hierarchically ordered macro-/mesoporous silica materials by using the polymer colloidal crystal and block copolymer P123 as the dual templates through the impregnation approach.

Nitrogen adsorption/desorption isotherms (Figure 6) of all HOPS samples synthesized by using prehydrolyzed precursor solution with different HCl amount exhibit similar type IV curves with pronounced H2 hysteresis loops due to the existence of irregular mesopores formed on the microspheres surface. The sharp capillary condensation steps occur at relative pressure of 0.6 − 0.7, indicating uniform mesopores. All samples have similar

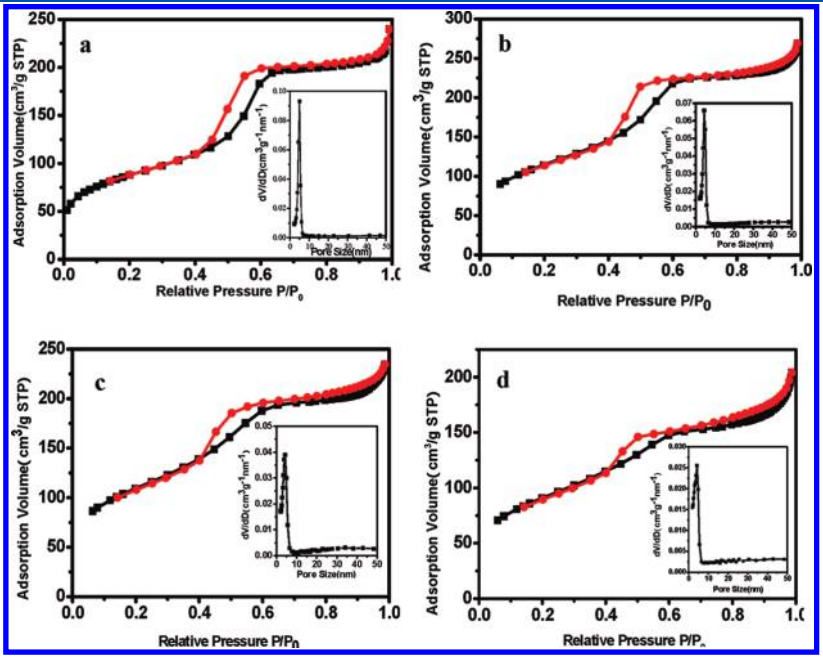

Figure 6. N_2 sorption isotherms and pore size distributions (inset) of the samples (a) HOPS-01-01, (b) HOPS-03-01, (c) HOPS-05-01, and (d) HOPS-08-01 prepared by using the precursor solution catalyzed by 2.0 M HCl solution of (a) 0.1, (b) 0.3, (c) 0.5, and (d) 0.8 g, and the same prehydrolysis time (1 h).

dx.doi.org/10.1021/cm103704s |*Chem. Mater.* 2011, 23, 2176–2184

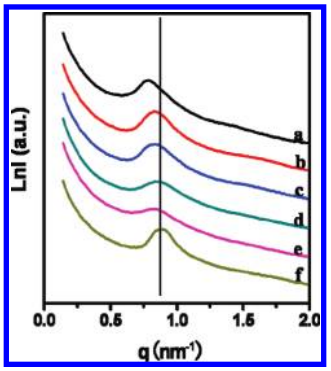

Figure 7. SAXS patterns of the samples: (a) HOPS-01-01, (b) HOPS-03-01, (c) HOPS-05-01, and (d) HOPS-08-01 prepared by using the precursor solution containing different amounts of 2.0 M HCl solution (a) 0.1, (b) 0.3, (c) 0.5, and (d) 0.8 g. The rehydrolysis time is the same, i.e., 1 h. (e) HOPS-08-10 and (f) HOPS-08-20 obtained with 0.8 g of 2.0 M HCl solution after the prehydrolysis for (e) 10 and (f) 20 h.

BET surface of about 330 m^2/g and pore volume of ~0.36 cm^3/g (Table 1), suggesting that the acidity of the precursor solution has little effect on the surface areas. The pore size distribution curves derived from the adsorption branches using the BJH model reveal the presence of relatively uniform mesopores in all selected samples (Table 1 and Figure 6 insets). The mean mesopore sizes of the samples range from 3.5−4.4 nm, showing a slight variation as the synthesis condition changes (Table 1). According to the small-angle X-ray scattering (SAXS) measurement results, all samples only exhibit a broad scattering peak at 0.8 nm^{-1}, indicating a relatively low periodicity of mesostructure (Figure 7), which is mainly due to the small domain of mesostructures formed in the interstitial voids of the colloidal crystals and the irregular alignment of large amount of mesopores on the spherical surface of the polymer sphere templates.[13]

3.3. Size-Selective Absorption of Biomolecules. Since the HOPS materials have numerous mesopores of 3.5−4.7 nm and 3D macropores of about 1.0 μm with variable window sizes of 0−200 nm, biomacromolecule absorption experiments were performed to study the application possibility of the HOPS materials for size selective absorption. We first investigated adsorption isotherms of the HOPS materials by using HOPS-08-01 and Cyt.c solutions with different concentrations at pH 9.5. With the increase of initial Cyt.c solution concentration, the adsorbed amount of Cyt.c on HOPS materials continuously increases from 11.3 to 36.5 mg/g and reaches an adsorption plateau with the maximum at about 37 mg/g (see Figure S3 in the Supporting Information). FT-IR spectra of the Cyt.c before and after adsorption on HOPS materials show no visible difference, implying that theprotein molecules are stable during the whole adsorption process at room temperature (see Figure S4 in the Supporting Information).

Because Bovine serum albumin (globular ellipsoid, 14 × 3.8 × 3.8 nm)[33] and cytochrome *c* (2.6 × 3.2 × 3.0 nm)[34] have different hydrodynamic size in solution, we used them as the model guest biomacromolecules for size-selective adsorption, and the sample HOPS-01−01 without macropore entrance and HOPS-08-01 with entrance of ~50 nm were used as absorbents to test their adsorption performance in mixed protein solution. The SDA-PAGE analysis (Figure 8) shows two bands in the lane of the mixture, indicating an adsorption of BSA (band 2) and Cyt. c solutions (band 1), respectively. Areas a, b, and c represent the

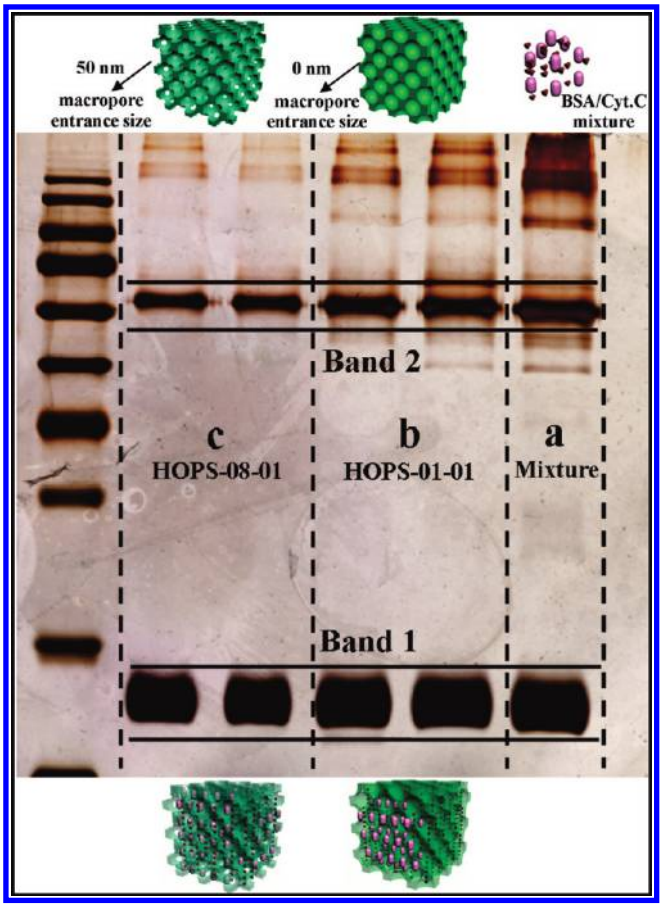

Figure 8. SDS-PAGE analysis results of (a) the mixture solution containing BSA and Cyt.c before the adsorption, (b) the mixed solution after the adsorption by the sample HOPS-01−01 without macropore entrance, and (c) HOPS-08−01 with 50 nm size macropore entrance.

initial mixture solution containing BSA and Cyt.c, that after the adsorption by HOPS-01-01 and HOPS-08-01, respectively. After the adsorption by HOPS-08-01 (area c), the width of band 2 in area c is reduced significantly compared with that in area a, clearly indicating a large adsorption capacity of HOPS-08-01 for BSA. However, for the sample HOPS-01-01 (area b), the width of band 2 reduces a little bit, suggesting a low adsorption capacity for BSA. Notably, the adsorption capacity of Cyt.c for the sample HOPS-01-01 is similar to that for HOPS-08−01, which suggests that the small protein molecules are adsorbed by the HOPS materials mainly through the mesopores. These results suggest that the HOPS-08-01 materials with large macropore entrances and mesopores can provide the access for both large guest objects and small sized molecules; while the HOPS-01-01 with closed macropores can exclude the large object (BSA) but allow small one (Cyt.c) to enter, implying a size-selective adsorption. Furthermore, quantitative measurements using UV−vis spectroscopy show that for BSA molecules, the sample HOPS-08-01 has much higher adsorption capacity (16.6 mg/g) than that (3.4 mg/g) of HOPS-01-01, whereas for Cyt.c protein, the samples HOPS-08-01 and HOPS-01-01 show a similar adsorption capacity of 37.4 and 36.8 mg/g, respectively. These results further indicate that the HOPS materials with small macropore entrances possess excellent size-selectivity for biomolecule adsorption. Therefore, by designing and engineering the pore

combination of the hierarchically porous materials, novel ordered porous materials can be created for size-selective absorption and enrichment, which is extremely important for diagnosis, drug delivery, and disease-relevant biomarkers screening.

4. CONCLUSION

In this paper, for the first time, we demonstrate a controlled synthesis of hierarchically ordered macro-/mesoporous silicate monoliths with adjustable macropore window sizes via a dual-templating approach, which combines colloidal crystal templating synthesis and amphiphilic triblock copolymer involved solvent evaporation-induced self-assembly process. It is found that the prehydrolysis time of the silica source, the concentration of acid and sintering conditions of colloidal crystal templates have influence on the macropore entrance size. The increase of HCl amount can enlarge the macropore window size from 0 to 50 nm. Prolonging the sol solution prehydrolysis time (1 to 20 h) can lead to a significant increase in macropore entrance (from 50 to 200 nm). Increasing the sintering temperature of the polymer colloidal crystal template to 90 °C can result in a large macropore window (150 nm). The obtained samples not only have 3D ordered macropores (~1.0 μm) with tunable entrance size but also possess 2D hexagonally packed mesopores of around 4.0 nm, high BET surface area (ca. 330 m^2/g), and large pore volume (~0.36 cm^3/g). Adsorption experiments indicate that the obtained hierarchically ordered porous silica monolithic materials exhibits excellent size selectivity for the adsorption in the mixture solution of BSA and Cyt.c. The controllable dual-template synthesis makes it possible to create hierarchically ordered macro-/mesoporous materials with adjustable macropore entrance sizes for various applications, such as selective adsorption and separation of biomolecules, drug delivery, molecular recognition, and screening disease-relevant biomarkers.

■ ASSOCIATED CONTENT

Supporting Information. Synthetic procedure for all the HOPS samples and the details of adsorption test, SEM images of samples prepared on the basis of polymer colloidal crystal treated with different sintering temperatures and different sintering time, IR spectra of the HOPS-01-01 sample for the different stages of the fabrication process, adsorption isotherms of Cyt.c on HOPS-08-01, IR spectra of Cyt.c before and after absorbed on HOPS-08−01, and SAXS patterns of various samples synthesized using different amounts of 2 M HCl and different prehydrolysis time of TEOS (PDF). This material is available free of charge via the Internet at http://pubs.acs.org.

■ AUTHOR INFORMATION

Corresponding Author

*E-mail: yhdeng@fudan.edu.cn; dyzhao@fudan.edu.cn.

■ ACKNOWLEDGMENT

This work was supported by NSF of China (2089012, 20721063, 20871030, and 21073040), State Key Basic Research Program of PRC (2006CB932302), Shanghai Leading Academic Discipline Project (B108), Shanghai Rising Star Program (08QA14010), Doctoral Program Foundation of State Education Commission of China (200802461013), and Science & Technology Commission of Shanghai Municipality (08DZ2270500). We are grateful to Professor C. H. Deng for assistance in protein adsorption and helpful discussion.

■ REFERENCES

(1) Diddams, P.; *Inorganic Supports and Catalysts*; Ellis Horwood: New York, 1992; pp 3−39.
(2) Sarrade, S. J.; Rios, G. M.; Carles, M. *Sep. Purif. Technol.* **1998**, *14*, 19.
(3) Beck, J. S.; Vartul, J. C.; Roth, W. J.; Leonowicz, M. E.; Kresge, C. T. *J. Am. Chem. Soc.* **1992**, *114*, 10834.
(4) Kresge, C. T.; Leonowicz, M. E.; Roth, W. J.; Vartuli, J. C.; Beck, J. S. *Nature* **1992**, *359*, 710.
(5) Davis, M. E. *Nature* **2002**, *417*, 813.
(6) Fan, J.; Yu, C. Z.; Gao, T.; Lei, J.; Tian, B. Z.; Wang, L. M.; Luo, Q.; Tu, B.; Zhou, W. Z.; Zhao, D. Y. *Angew. Chem., Int. Ed.* **2003**, *42*, 3146.
(7) Yan, X. X.; Yu, C. Z.; Zhou, X. F.; Tang, J. W.; Zhao, D. Y. *Angew. Chem., Int. Ed.* **2004**, *43*, 5980.
(8) Huo, Q.; Margolese, D. I.; Ciesla, U.; Demuth, D. G.; Stucky, G. D. *Chem. Mater.* **1994**, *6*, 1176.
(9) Brinker, C. J.; Scherer, G. W.; *Sol−Gel Science*; Academic: New York, 1990.
(10) Tian, B.; Yang, H.; Liu, X.; Xie, S.; Yu, C.; Fan, J.; Tu, B.; Zhao, D. Y. *Chem. Commun.* **2002**, *17*, 1824.
(11) Yang, P. D.; Zhao, D. Y.; Margolese, B.; Chmelka, F.; Stucky, G. D. *Nature* **1998**, *396*, 152.
(12) Ma, G. Q.; Yan, X.; Fan, J. etc. *J. Am. Chem. Soc.* **2010**, *132*, 9596−9597.
(13) Deng, Y. H.; Liu, C.; Yu, T.; Liu, F.; Zhang, F. Q.; Zhao, D. Y. *Chem. Mater.* **2007**, *19*, 3271–3277.
(14) Liu, J.; Cai, Y.; Deng, Y. H.; Sun, Z. K.; Gu, D.; Tu, B.; Zhao, D. Y. *Microporous Mesoporous Mater.* **2010**, *130*, 26–31.
(15) Holland, B. T.; Blanford, C. F.; Stein, A. *Science* **1998**, *281*, 538.
(16) Yang, S. M.; Coombs, N.; Ozin, G. A. *Adv. Mater.* **2000**, *12*, 1940.
(17) Imhof, A.; Pine, D. J. *Nature* **1997**, *389*, 948.
(18) Sen, T.; Tiddy, G. J. T.; Casci, J. L.; Anderson, M. W. *Angew. Chem., Int. Ed.* **2003**, *42*, 4649–4653.
(19) Coppens, M. O.; Sun, J. H.; Maschmeyer, T. *Catal. Today* **2001**, *69*, 331.
(20) Zhao, D. Y.; Feng, J. L.; Huo, Q. S.; Melosh, N.; Fredrickson, G. H.; Chmelka, B. F.; Stucky, G. D. *Science* **1998**, *279*, 548.
(21) Holland, B. T.; Abrams, L.; Stein, A. *J. Am. Chem. Soc.* **1999**, *121*, 4308.
(22) Holland, B. T.; Blanford, C. F.; Do, T. *Chem. Mater.* **1999**, *11*, 795.
(23) Danumah, C.; Vaudreuil, S.; Bonneviot, L.; Bousmina, M.; Giasson, S.; Kaliaguine, S. *Microporous. Mesoporous Mater.* **2001**, *44−45*, 241.
(24) Zhou, Y.; Antonietti, M. *Chem. Commun.* **2003**, 2564.
(25) Oh, C. G.; Baek, Y.; Ihm, S. K. *Adv. Mater.* **2005**, *17*, 270.
(26) Yuan, Z. Y.; Ren, T. Z.; Vantomme, A.; Sun, B. L. *Chem. Mater.* **2004**, *16*, 5096.
(27) Smatt, J. H.; Schunk, S.; Linden, M. *Chem. Mater.* **2003**, *15*, 2354.
(28) Li, C. Z.; He, J. H. *Langmuir* **2006**, *22*, 2827.
(29) Villaescusa, L. A.; Mihi, A.; Rodriguez, I.; Garcia-Bennett, A. E.; Miguez, H. *J. Phys. Chem. B* **2005**, *109*, 19643.
(30) Li, F.; Wang, Z. Y.; Ergang, N. S; Fyfe, C. A.; Stein, A. *Langmuir* **2007**, *23*, 3996.
(31) Sen, T.; Tiddy, G. J. T.; Casci, J. L.; Anderson, M. W. *Chem. Mater.* **2004**, *16*, 2044.
(32) Deng, Y. H.; Liu, C.; Liu, J.; Zhang, F.; Yu, T.; Zhang, F. Q.; Gu, D.; Zhao, D. Y. *J. Mater. Chem.* **2008**, *18*, 408.
(33) Shirahama, H.; Suzawa, T. *Colloid Polym. Sci.* **1985**, *263*, 141.
(34) Zhang, M.; Wu, Y. P.; Feng, X. Z.; He, X. W.; Chen, L. X.; Zhang, Y. K. *J. Mater. Chem.* **2010**, *20*, 5835.

(35) Vinu, A.; Miyahara, M.; Ariga, K. *J. Phys. Chem. B* **2005**, *109*, 6436.
(36) Vinu, A.; Murugesan, V.; Tangermann, O.; Hartmann, M. *Chem. Mater.* **2004**, *16*, 3056.
(37) Vinu, A.; Murugesan, V.; Hartmann, M. *J. Phys. Chem. B* **2004**, *108*, 7323.
(38) Vinu., A.; Gokulakrishnan, N.; Balasubramanian, V. V.; Alam, S.; Kapoor, M. P.; Ariga, K.; Mori, T. *Chem.—Eur. J.* **2008**, *14*, 11529.
(39) Vinu, A.; Hossain, K. Z.; Srinivasu, P.; Miyahara, M.; Anandan, S.; Gokulakrishnan, N.; Mori, T.; Ariga, K.; Balasubramanian, V. V. *J. Mater. Chem.* **2007**, *17*, 1819.